

---

## The role of $H_3^+$ in planetary atmospheres

Steven Miller, Nick Achilleos, Gilda E. Ballester, Thomas R. Geballe, Robert D. Joseph, Renée Prangé, Daniel Rego, Tom Stallard, Jonathan Tennyson, Laurence M. Trafton and J. Hunter Waite, Jr

*Phil. Trans. R. Soc. Lond. A* 2000 **358**, 2485-2502

doi: 10.1098/rsta.2000.0662

---

### Email alerting service

Receive free email alerts when new articles cite this article - sign up in the box at the top right-hand corner of the article or click [here](#)

---

To subscribe to *Phil. Trans. R. Soc. Lond. A* go to:  
<http://rsta.royalsocietypublishing.org/subscriptions>

---

# The role of $\text{H}_3^+$ in planetary atmospheres

BY STEVEN MILLER<sup>1†</sup>, NICK ACHILLEOS<sup>1†</sup>, GILDA E. BALLESTER<sup>2</sup>,  
 THOMAS R. GEBALLE<sup>3</sup>, ROBERT D. JOSEPH<sup>4</sup>, RENÉE PRANGÉ<sup>5</sup>,  
 DANIEL REGO<sup>5</sup>, TOM STALLARD<sup>1†</sup>, JONATHAN TENNYSON<sup>1†</sup>,  
 LAURENCE M. TRAFTON<sup>6†</sup> AND J. HUNTER WAITE JR<sup>7</sup>

<sup>1</sup>*Department of Physics and Astronomy, University College London,  
 Gower Street, London WC1E 6BT, UK*

<sup>2</sup>*Department of Atmospheric, Oceanic and Space Sciences,  
 University of Michigan, 2455 Hayward Street,  
 Ann Arbor, MI 48109, USA*

<sup>3</sup>*Gemini Observatory, 670 North A'ohoku Place, Hilo, HI 96720, USA*

<sup>4</sup>*Institute for Astronomy, University of Hawaii,  
 Woodlawn Drive, Honolulu, HI 96822, USA*

<sup>5</sup>*Institut d'Astrophysique Spatiale, UMR-CNRS 120, Bâtiment 121,  
 Université de Paris XI, 91405 Orsay Cedex, France*

<sup>6</sup>*McDonald Observatory and Department of Astronomy,  
 University of Texas at Austin, Austin, TX 78712, USA*

<sup>7</sup>*Department of Space Science, Southwest Research Institute,  
 PO Box 28510, San Antonio, TX 78228, USA*

Spectroscopic studies of the upper atmospheres of the giant planets using infrared wavelengths sensitive to the  $\text{H}_3^+$  molecular ion show that this species plays a critical role in determining the physical conditions there. For Jupiter, we propose that the recently detected  $\text{H}_3^+$  electrojet holds the key to the mechanism by which the equatorial plasma sheet is kept in (partial) co-rotation with the planet, and that this mechanism also provides a previously unconsidered source of energy that helps explain why the jovian thermosphere is considerably hotter than expected. For Saturn, we show that the  $\text{H}_3^+$  auroral emission is *ca.* 1% of that of Jupiter because of the lower ionospheric/thermospheric temperature and the lower flux of ionizing particles precipitated there; it is probably unnecessary to invoke additional chemistry in the auroral/polar regions. For Uranus, we report further evidence that its emission intensity is controlled by the cycle of solar activity. And we propose that  $\text{H}_3^+$  emission may just be detectable using current technology from some of the giant *extra-solar planets* that have been detected orbiting nearby stars, such as Tau Bootes.

**Keywords:** giant planets; atmospheres; ionospheres;  
 thermospheres; aurorae; exoplanets

## 1. Introduction

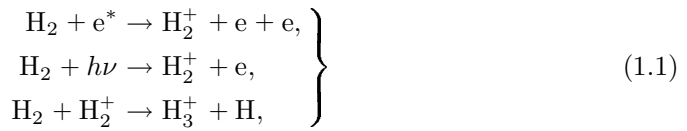
The accidental discovery of emission from  $\text{H}_3^+$  in the infrared spectrum of Jupiter's aurorae in 1988 (Drossart *et al.* 1989) has opened up a decade of investigations

† Visiting observer on the NASA Infrared Telescope Facility (IRTF), which is operated for NASA by the University of Hawaii Institute for Astronomy.

making use of this fundamental ion as a probe of the ionospheres of the outer planets.  $\text{H}_3^+$  had been proposed as a constituent of this atmospheric region a quarter of a century before its eventual detection (Gross & Rasool 1964), and its presence had been inferred from Voyager II measurements of the jovian magnetosphere (Hamilton *et al.* 1980). But, in 1988, no one could predict just how useful this ion would prove to be as a physical and chemical indicator, nor quite how important it would turn out to be in determining how the upper atmosphere of Jupiter and its fellow giants behaved.

Studies presented elsewhere in this issue explain how infrared imaging, using wavelengths sensitive to  $\text{H}_3^+$ , has been used to elucidate key parameters in the jovian magnetic field, and to highlight the highly energetic electromagnetic interactions between Jupiter and its moons, particularly Io (Connerney & Satoh, this issue). Our contribution looks mainly at the use of  $\text{H}_3^+$  infrared spectroscopic studies of the outer planets. It discusses the role that  $\text{H}_3^+$  plays in determining the thermal structure of the upper atmospheres of these giants and the more recent use of Doppler-shifted lines to probe the dynamics of the polar regions of Jupiter. And it looks ahead to a future in which the planetary supergiants that have been detected orbiting stars close to our own Solar System (see, for example, Mayor & Queloz 1995; Marcy & Butler 1996; Cameron *et al.* 1999) might similarly be probed.

There have been many successful attempts to model giant planetary ionospheres (see, for example, Gross & Rasool 1964; Atreya & Donahue 1976; Waite *et al.* 1983; McConnell & Majeed 1991; Kim *et al.* 1992) to complement terrestrial and *in situ* measurements. In these models,  $\text{H}_3^+$  is produced by chemical reactions, such as



where  $e^*$  represents energetic electrons precipitating along magnetic fieldlines, and  $h\nu$  is solar extreme ultraviolet (EUV) radiation. The ion is destroyed by



Until recently, such models were all one dimensional, so that the dynamical production and distribution of this ion on a planet rotating under solar radiation could not be reproduced. Achilleos *et al.* (1998), however, have now produced a three-dimensional, fully coupled model of the jovian thermosphere/ionosphere. (The thermosphere, consisting of neutral gas, and the ionosphere, consisting of plasma, physically coexist for the giant planets in the pressure region from *ca.*  $1 \mu\text{bar}$  to *ca.*  $0.01 \text{nbar}$ .) Here we shall make considerable use of this jovian ionosphere model (known as JIM) to interpret the results of  $\text{H}_3^+$  spectroscopic studies. We shall also consider the possibility of extending JIM to model other planets.

## 2. Jupiter

### (a) *Some outstanding questions*

Apart from the solar wind, the jovian magnetosphere is the largest structure in our Solar System. In the Sunward direction, it extends *ca.* 7 million km, while the mag-

netotail stretches out to the orbit of Saturn (and may sometimes even envelop that planet). Unlike the terrestrial magnetosphere, which is fuelled by the solar wind, the predominant source of plasma in the jovian system is the Galilean moon Io, whose volcanoes pump out approximately 1 to a few tonnes of material per second (J. Spencer, personal communication). This gives rise to a dense plasma region along the orbit of Io, known as the Io plasma torus, and an extended equatorial plasma sheet, which rotates along with the planet out to about 20 jovian radii ( $R_J = 71\,492$  km); partial co-rotation probably extends for up to 50–60  $R_J$ . The mechanism by which the plasma sheet is kept co-rotating, proposed by Hill (1979), involves the transfer of rotational energy from Jupiter by a kind of electromagnetic friction. Co-rotation is maintained by currents flowing outwards through the sheet itself, and along magnetic fieldlines that connect the orbit of Io (upwards from the planet) and the outer edge of the co-rotating plasma (downwards towards the planet) to the atmosphere; the circuit is closed by means of an equatorward current flowing through the ionosphere itself. In the steady state, it is possible to show that this mechanism must be transferring between 1 and  $10 \times 10^{12}$  J of rotational kinetic energy per second from Jupiter to the plasma sheet; this is a similar, if somewhat smaller, amount of energy to the tidal energy Jupiter supplies to Io to produce its volcanic activity. (There is no chance of Jupiter's angular momentum reservoir being exhausted, however, since it is *ca.*  $6 \times 10^{34}$  J.) Just how this energy transfer process works in detail is still in question.

Another such question involves the rather high temperatures detected in the jovian upper atmosphere. Voyager found the ionospheric temperature to be *ca.* 1000 K, and this high temperature was confirmed by Drossart *et al.*'s (1989) auroral measurement of 1100 K. Subsequent  $\text{H}_3^+$  auroral infrared measurements have resulted in temperatures between 670 K (Oka & Geballe 1990) and 1250 K (Maillard *et al.* 1990), with 'ambient' temperatures between 800 and 1100 K (Miller *et al.* 1990; Lam *et al.* 1997*a*). One key finding was that  $\text{H}_3^+$  emission showed the gas was in 'quasi-thermal equilibrium' (Miller *et al.* 1990): that means that this ion and its emission are sensitive to temperatures prevailing in the ionosphere/thermosphere in a way that UV emission is not. The auroral temperatures may be explicable by the energy influx required to power Jupiter's ultraviolet aurorae. What are more difficult to explain are the non-auroral temperatures, shown to be between 700 and 950 K (de Bergh *et al.* 1992; Miller *et al.* 1997), several hundred degrees higher than might be expected from the solar influx to the ionosphere/thermosphere of just  $60 \mu\text{W m}^{-2}$  (Atreya 1986). Waite *et al.* (1983) proposed that thermospheric winds might be involved in distributing energy from the auroral regions to lower latitudes to account for these high temperatures. But, again, just how?

We shall argue that  $\text{H}_3^+$  holds the key to explaining both the temperature structure of the jovian upper atmosphere *and* the process by which planetary angular momentum is transferred to the equatorial plasma sheet. But first we need to look at some considerations of the overall energy balance, and just where that energy is located.

### (b) Energy considerations

Although they are inevitably linked together, it is useful to consider the ionospheric/thermospheric region of the jovian atmosphere as being divided into an auroral/polar region and a non-auroral region, which encompasses all latitudes lower than

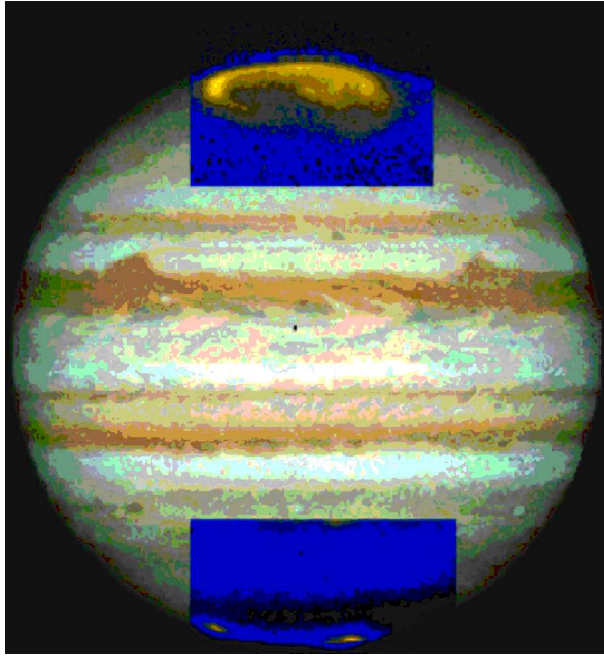


Figure 1. Infrared images of the jovian aurorae taken at  $3.953\ \mu\text{m}$ , the wavelength of the  $\text{H}_3^+ \nu_2 Q(1, 0^-)$  line, superimposed on a visible image of Jupiter. The infrared images were taken using the NASA IRTF.

that traced out by the magnetic fieldline footprint of Io, the  $5.9R_J$  footprint. (Magnetic fieldline footprints are designated by the distance from the centre of the planet at which they cross the magnetic equatorial plane.) Strong ultraviolet aurorae have been known to emanate from Jupiter for many years (see Livengood *et al.* (1992) for details). Jupiter is also known to have a UV airglow (Clarke *et al.* 1980, 1981).

Until recently, there was little information about the spatial distribution of the auroral/polar emission. But Hubble Space Telescope images (see, for example, Clarke *et al.* 1996, 1998; Ballester *et al.* 1996; Prangé *et al.* 1997, 1998) show that this emission region consists of a main, rather narrow, auroral oval, with structured emission at higher latitude and inside of the polar cap, and a belt of emission at lower latitudes that includes trails corresponding to the footprints of Io and, perhaps, other Galilean moons. This structure is mirrored in the infrared  $\text{H}_3^+$  images of Jupiter's polar regions (see figure 1; see also Satoh *et al.* (1996) and Satoh & Connerney (1999)), indicating that the production of this ion closely follows the production of UV emission. There is additionally mid-to-low (MTL)  $\text{H}_3^+$  emission (Miller *et al.* 1997) extending equatorwards from the Io orbital footprint.

The UV auroral/polar output has variously been estimated at a few  $\times 10^{12}$  W (Clarke *et al.* 1996) to more than  $10^{13}$  W (see Livengood *et al.* (1992) for a fuller discussion). Based on an efficiency of *ca.* 10%, energy inputs have then been estimated to be between  $10^{13}$  and  $10^{14}$  W; this input energy comes in the form of particles: mainly keV electrons precipitating along fieldlines into the atmosphere. But two recent studies (Satoh & Connerney 1999; Rego *et al.* 2000) have both shown that in the auroral/polar region, the atmosphere above the  $2\ \mu\text{bar}$  homopause—where it

consists of hydrogen and helium species only, and where  $H_3^+$  is produced—absorbs only a few  $\times 10^{12}$  W. (The remainder of this input precipitation energy is presumably absorbed at or below the homopause, consistent with the fact that the UV aurorae are usually accompanied by hydrocarbon absorption features.) There appears to be further precipitation in the MTL latitude regions required to account for X-ray emission (Waite *et al.* 1997) and the MTL  $H_3^+$  emission noted by Miller *et al.* (1997). This latter has been calculated to be  $0.65 \times 10^{12}$  W per hemisphere (Rego *et al.* 2000). Gravity waves have been suggested as a source of energy to the ionosphere/thermosphere (Yelle *et al.* 1996; Young *et al.* 1997), in an attempt to explain the low-latitude temperature profile found by the Galileo probe (Seiff *et al.* 1997), although doubt has recently been cast on the efficacy of this process (Matcheva & Strobel 1999). In addition, the insolation available to the jovian ionosphere/thermosphere— $60 \mu\text{W m}^{-2}$  in the EUV—translates to *ca.*  $10^{12}$  W planet-wide. Overall, therefore, the energy absorbed by the ionosphere/thermosphere above the homopause is *ca.*  $5 \times 10^{12}$  W (Rego *et al.* 2000).

The effect of these various energy inputs must be to heat up the ionosphere, unless they are somehow re-radiated, or conducted and/or convected (unlikely above the homopause, which, by definition, is a region where convection ceases) away. The ionosphere/thermosphere is a poor conductor of heat, which leaves radiation. According to studies of the jovian UV electroglow, this feature can probably account for almost all of the  $10^{12}$  W of EUV insolation (Feldman *et al.* 1993; Liu & Dalgarno 1996). That still leaves *ca.*  $4 \times 10^{12}$  W to be considered. Since it is not a black body, the ionosphere will heat up until some species starts to radiate efficiently. The dominant atmospheric species, molecular hydrogen, is a poor radiator at infrared wavelengths as it has neither a permanent nor a vibrationally induced dipole moment. But at temperatures between 700 and 1100 K,  $H_3^+$  emits between  $5 \times 10^{-21}$  W  $\text{sr}^{-1}$  molecule $^{-1}$  and  $5 \times 10^{-20}$  W  $\text{sr}^{-1}$  molecule $^{-1}$ . Although its density is rarely above  $10^{11}$  m $^{-3}$ , compared with  $[H_2]$  *ca.*  $10^{18}$  m $^{-3}$  at the  $\mu\text{bar}$  level, this high radiative efficiency is enough to make  $H_3^+$  emission the predominant cooling mechanism in both the auroral/polar (Satoh & Connerney 1999; Rego *et al.* 2000) and non-auroral ionosphere/thermosphere (Waite *et al.* 1997). Indeed, it is clear that  $H_3^+$  emission may account for more than the *ca.*  $5 \times 10^{12}$  W of input energy considered so far: the findings of Rego *et al.* (2000) could be interpreted as showing  $H_3^+$  emitting up to  $8 \times 10^{12}$  W planet-wide.

### (c) *The auroral electrojet*

Recently, Rego *et al.* (1999) have detected an ion wind flowing around the auroral oval of Jupiter, by means of a Doppler-shifted  $H_3^+$  spectrum (figure 2). This auroral electrojet that these authors detected was unusually rapid, associated with velocities of *ca.*  $3 \text{ km s}^{-1}$ , close to or just exceeding the local thermospheric speed of sound, and they attributed their detecting it to an unusually energetic ‘auroral event’. The electrojet results naturally from the mechanism proposed by Hill (1979) to explain the way in which plasma sheet co-rotation is enforced via currents flowing outwards in the plasma sheet and along the fieldlines that connect the outer (downward current) and inner (upward current) parts of the plasma sheet to the ionosphere. The current closes through the ionosphere, where fields of a few hundred kV to a few MV may be produced. The resulting combination of Jupiter’s magnetic field,  $\mathbf{B}$ , being normal



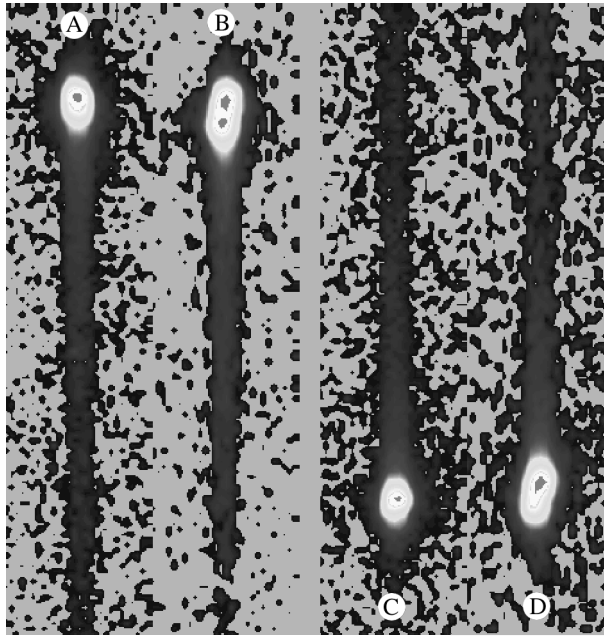


Figure 2. Pole-to-equator spectral images of Jupiter at  $3.953\ \mu\text{m}$ , the wavelength of the  $\text{H}_3^+ \nu_2 Q(1, 0^-)$  line, obtained using CSHELL, the facility echelle spectrometer on the NASA IRTF. The spectrometer slit is aligned jovian north–south along the central meridian. North is at the top. (a) North pole to equator, 16 July 1996; (b) north pole to equator, 8 August 1997; (c) south pole to equator, 14 July 1996; (d) south pole to equator, 8 September 1997. In the 1996 spectra, only one intensity peak is visible, but in the 1997 data, a double peak is seen as the result of an ‘auroral event’. The outermost peak is also clearly Doppler shifted (red in the north, blue in the south) as the slit cuts the auroral electrojet.

to the planet’s surface, and the equatorward electric field,  $\mathbf{E}$ , produces an  $\mathbf{E} \times \mathbf{B}$  force that drives ions (and electrons) around the auroral oval in the clockwise, anti-co-rotational, sense. Follow-up studies by T. Stallard *et al.* (unpublished data) show that electrojet velocities of  $ca. 500\ \text{m s}^{-1}$  may routinely be detected. Achillesos *et al.* (2000) have modelled the production of electrojets using JIM for a variety of equatorial, transauroral voltages; they found that equatorward fields of  $ca. 2\ \text{MV}$  produce ion velocities of  $ca. 500\ \text{m s}^{-1}$ .

What is even more significant, however, is that the modelling shows that, as the velocity of the ions increases, they entrain the neutral thermosphere in the auroral oval, producing velocities that reach between 20% and 40% of the ions (figure 3). Such neutral entrainment in the auroral electrojet is associated with a large amount of energy: for the case of a 2 MV potential,  $ca. 8 \times 10^{15}\ \text{J}$  are associated with the neutrals as they stream counter to the planet’s direction of diurnal rotation. This motion must be associated with considerable atmospheric ‘friction’, as entrained gas sweeps past the atmosphere outside of the electrojet region, which is in co-rotation with the planet. It is this friction that provides the mechanism to impart the rotational energy of the planet to the plasma sheet. To find out how much frictional energy was being transferred, we switched off the equatorward field in JIM; this is equivalent to instantaneously bringing the plasma sheet into perfect

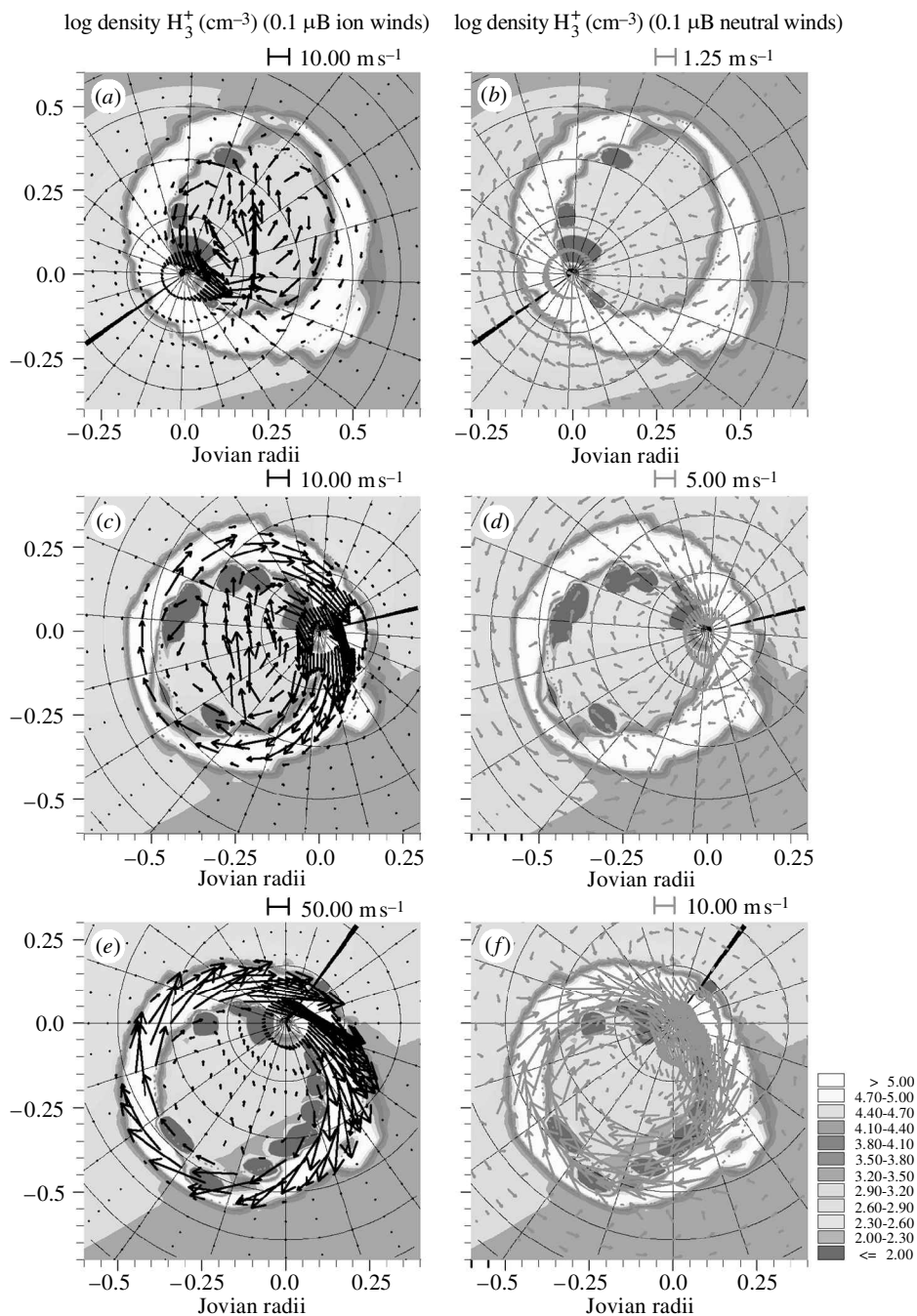


Figure 3. Effect of increasing the equatorward potential across the jovian auroral oval. Voltages increase from 10 kV ((a), (b)), through 100 kV ((c), (d)), to 1 MV ((e), (f)). Ion winds are shown on the left, neutral winds on the right. (a), (b)  $\lambda_{\text{III}} = 304$  (noon); time is 3.84 jovian days. (c), (d)  $\lambda_{\text{III}} = 104$  (noon); time is 4.29 jovian days. (e), (f)  $\lambda_{\text{III}} = 144$  (noon); time is 4.40 jovian days.



co-rotation, while shutting down the mechanism by which plasma drifts outwards from the orbit of Io. The results showed that the energy of the neutral atmosphere entrained in the electrojet was dissipated with a half-life of *ca.* 1000 s, corresponding to an overall energy input to the atmosphere of *ca.*  $8 \times 10^{12}$  W. In the 'steady' state of outward drift in the plasma sheet and non-perfect co-rotation, this energy—or some fraction of it—is available to the upper atmosphere as a further—and previously unconsidered—source of heating.

#### (d) Summary

From the foregoing discussion it is clear that  $\text{H}_3^+$  plays a vital role in the physical conditions prevailing in Jupiter's ionosphere/thermosphere. It is the main coolant in both the auroral/polar and non-auroral regions, and the fact that its strong emission comes in at temperatures between 700 and 1100 K helps explain why temperatures in this range are consistently found above the jovian homopause.  $\text{H}_3^+$  is also pivotal in the mechanism by which the rotational energy of the planet is transferred to the equatorial plasma sheet *and* made available for heating the upper atmosphere.

One area not considered here is the role that  $\text{H}_3^+$  plays in the network of chemical reactions that occur in the jovian atmosphere. Models of the ionosphere/thermosphere show the concentration of this ion falling off rapidly at the homopause, even in the auroral/polar regions, despite the continuing presence of precipitating electrons with enough energy to ionize molecular hydrogen. This die off is due to reactions with, primarily, hydrocarbons occurring at or just below the  $\mu\text{bar}$  homopause. These reactions may be important in initiating the formation of more complex hydrocarbons, and other species. It would, therefore, be extremely interesting to be able to probe such processes using infrared spectroscopic observations; to date, however, no successful observations of jovian hydrocarbon ions have been made. But it may still be that the most important contribution that  $\text{H}_3^+$  makes to the chemistry below the homopause is in providing H atoms resulting from dissociative recombination (reaction (1.2)), as proposed by Prinn & Owen (1976).

### 3. The other giant planets

While  $\text{H}_3^+$  emission from Jupiter has received by far and away the most attention, this molecule is also known on Saturn (Geballe *et al.* 1993) and Uranus (Trafton *et al.* 1993), although studies of Neptune have failed to reveal its presence there. As in so many of their properties, while comparisons may be drawn,  $\text{H}_3^+$  studies reveal that each of the planets is different, a product of its own unique circumstances.

#### (a) Saturn

When  $\text{H}_3^+$  emission was first detected from Saturn by Geballe *et al.* (1993), two questions immediately came to mind: why was it so weak—only *ca.* 1% of the jovian auroral emission (see figure 4)—given that Saturn was of similar size to Jupiter ( $R_S \sim 60\,000$  km) and that its exposure to the solar wind should only be down by about a factor of four as a result, mainly, of the difference in distance from the Sun; and what was the distribution of the ion across the planet? Geballe *et al.*'s (1993) spatial resolution was *ca.*  $3''$ , and they were not able to distinguish between auroral enhancements at the poles and the effect that limb brightening might have

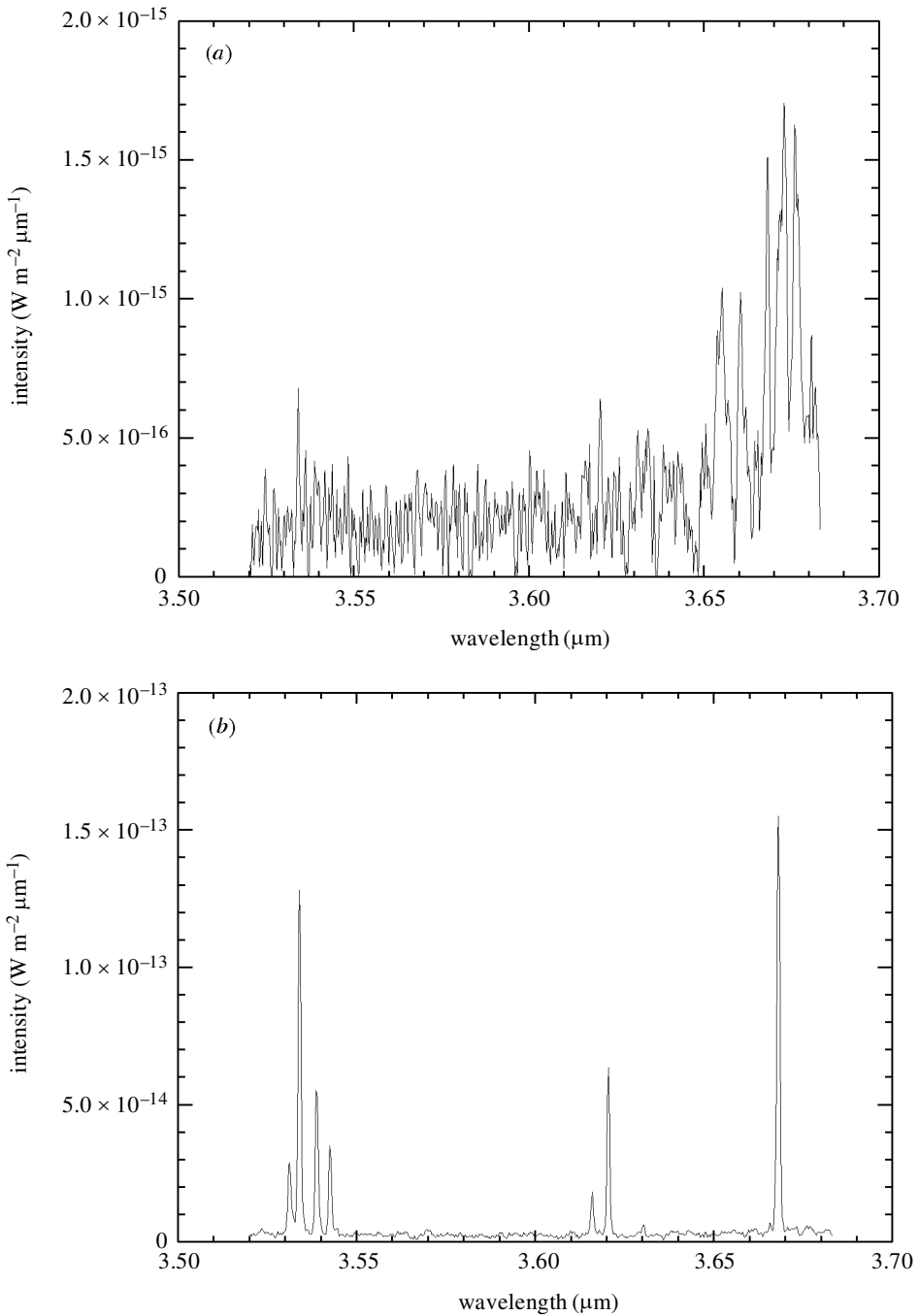


Figure 4.  $\text{H}_3^+$   $\nu_2$  spectra of Saturn (a) and Jupiter (b) obtained on the night of 17 September 1999, using CGS4, the facility echelle spectrometer on UKIRT.

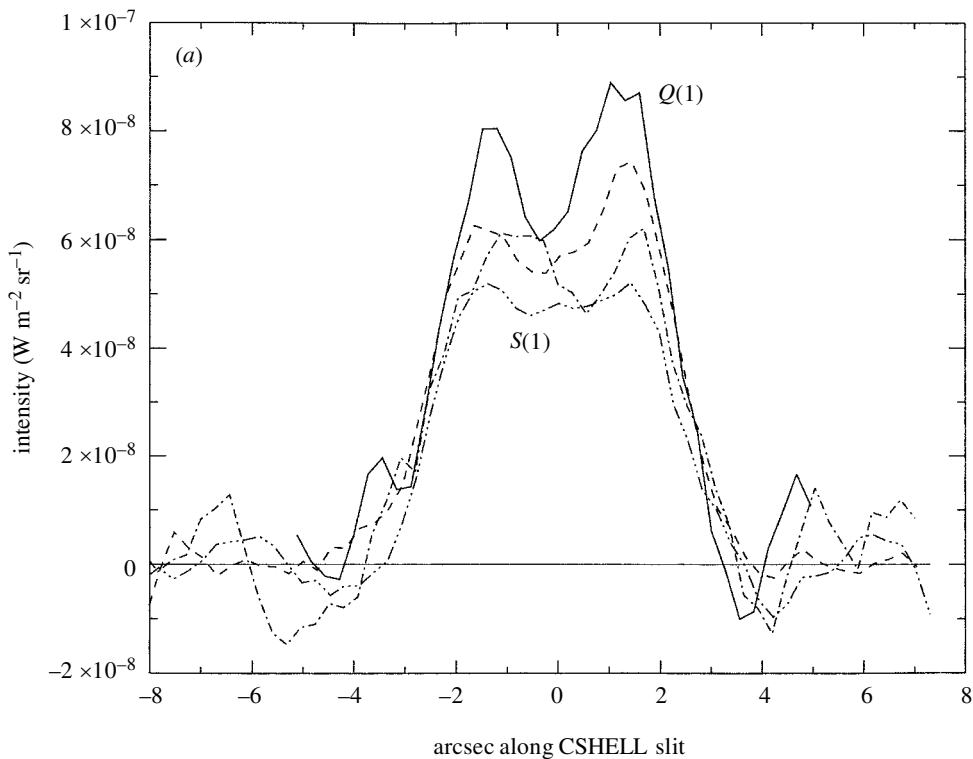


Figure 5. Emission profiles of  $\text{H}_2$  (a) and  $\text{H}_3^+$  (b) across the disc of Uranus obtained on the NASA IRTF using CSHELL. The profiles in (a) were obtained during August 1994, and those in (b) during May 1993. For (a), the solid line labelled  $Q(1)$  is the ( $v = 1 \rightarrow 0$ )  $Q(1)$  at  $2.41 \mu\text{m}$ ; the three broken lines are separate measurements of the ( $v = 1 \rightarrow 0$ )  $S(1)$  transition at  $2.12 \mu\text{m}$ .

on a uniformly emitting disc. These workers deduced an ionospheric temperature of *ca.* 800 K from their spectrum. This was in accordance with the top end of the 600–800 K range obtained by Atreya *et al.* (1984), but much higher than the 420 K that Majeed & McConnell (1996) required to fit radio occultation radio densities.

Recently, a new pole-to-pole emission profile of Saturn has been obtained (Stallard *et al.* 1999). This shows that  $\text{H}_3^+$  emission on Saturn is similar to that on Jupiter, in that it is concentrated in circum-polar auroral regions, answering the second of the questions raised by Geballe *et al.* (1993). Using the temperature of 800 K deduced by Geballe *et al.* (1993), Stallard *et al.* (1999) also estimated that the total  $\text{H}_3^+$  emission from Saturn was between  $1.2$  and  $3.6 \times 10^{11}$  W; this compares with the UV emissions, which range from a few  $\times 10^{10}$  W to as little as  $10^8$  W (Trauger *et al.* 1998). To explain the low level of  $\text{H}_3^+$  emission compared with Jupiter, Stallard *et al.* (1999) raised the possibility that chemical depletion of the ion as a result of reactions with hydrocarbons or water might be occurring; they also queried the temperature suggested by Geballe *et al.* (1993).

Figure 4 shows spectra taken of the southern polar regions of Saturn (figure 4a) and Jupiter (figure 4b) on the same night in September 1999. Lines clearly visible in Jupiter are present in the Saturn spectrum with slightly less than 1% of the jovian intensity. The Jupiter spectrum was fitted with a temperature of 900 K and

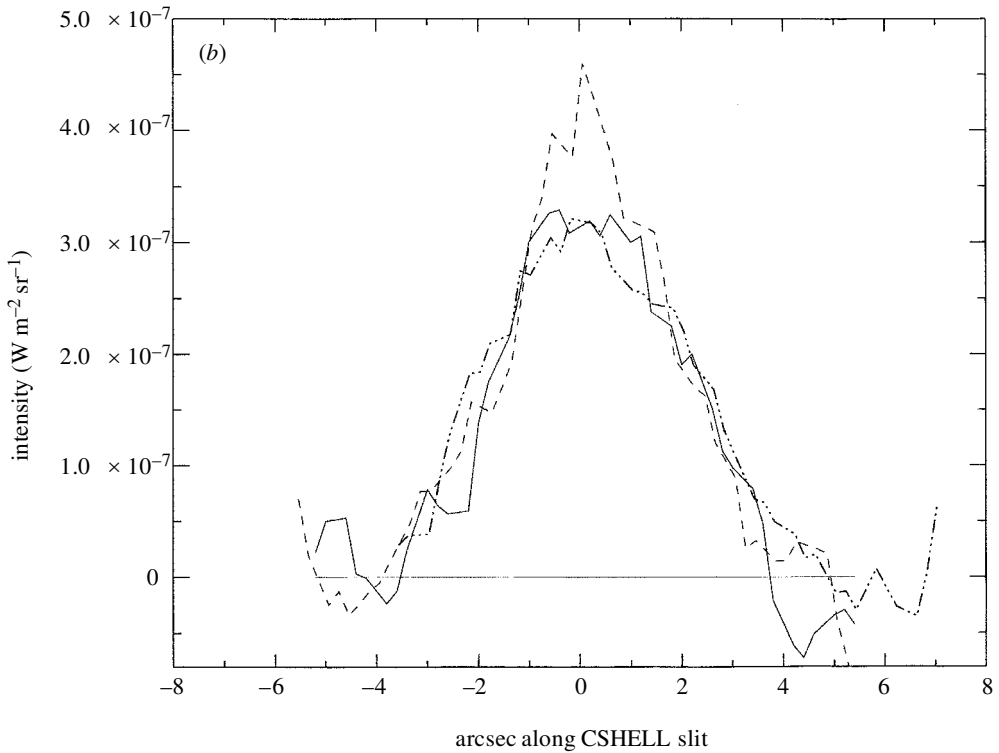


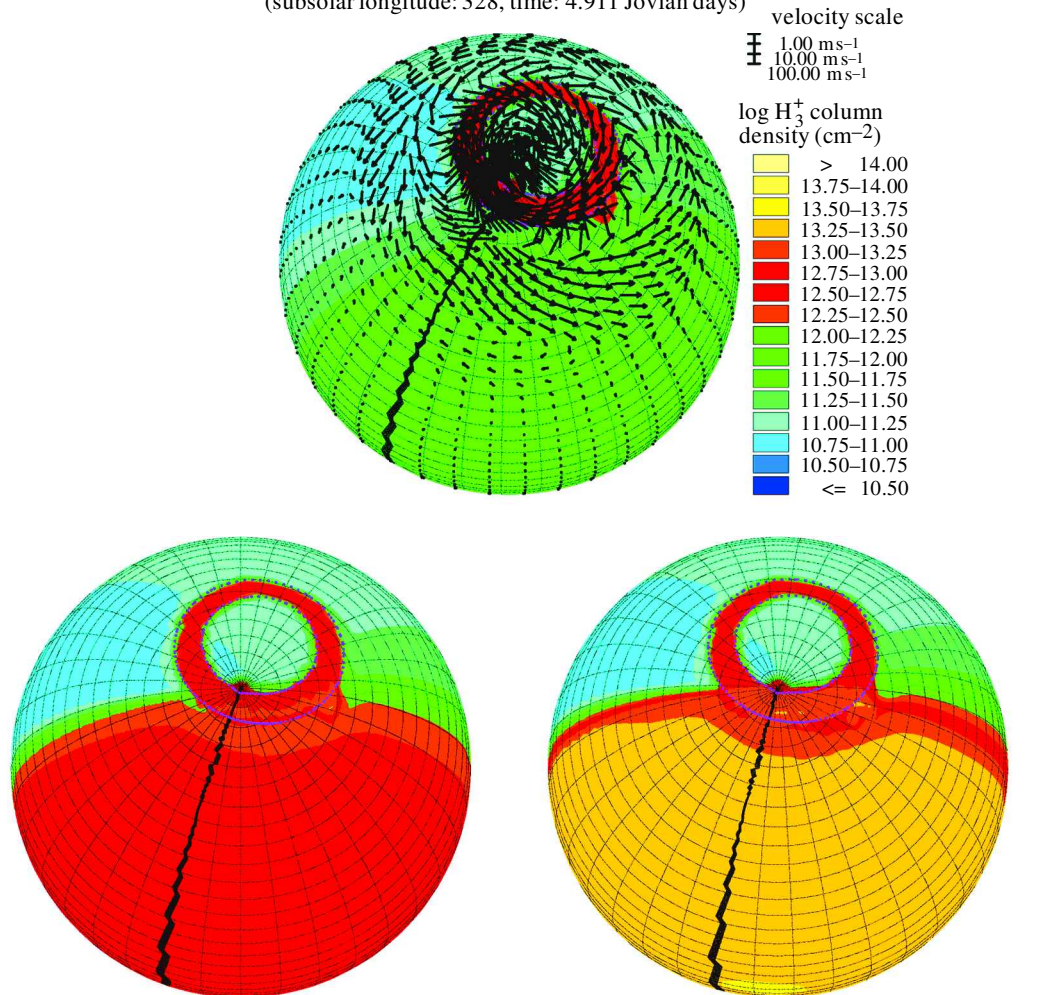
Figure 5. (Cont.)

a column density,  $N(\text{H}_3^+)$ , of  $6.6 \times 10^{16} \text{ m}^{-2}$ . For Saturn, the figures are  $T = 600 \text{ K}$  and  $N(\text{H}_3^+) = 2.8 \times 10^{15} \text{ m}^{-2}$ . The estimated area of the auroral emitting region is  $ca. 10^{15} \text{ m}^2$  (from Trauger *et al.* 1998), and, taking the  $\text{H}_3^+$  per molecule emission from Neale *et al.* (1996), total emission from the cronian southern auroral region is  $ca. 4 \times 10^{10} \text{ W}$ ; if the northern auroral emission is the same, and allowing for some emission from the body of the planet, the total emission from Saturn is  $ca. 10^{11} \text{ W}$ . This is in accord with the lower limit deduced by Stallard *et al.* (1999), and is  $ca. 2\%$  of the total jovian emission.

The lower cronian temperature means that each  $\text{H}_3^+$  molecule emits, on average,  $ca. 10\%$  of the radiation it does on Jupiter. Moreover, the UV results show that energy inputs into the ionosphere/thermosphere of Saturn are at least two orders of magnitude less than Jupiter, and possibly even lower. Since the JIM model shows that the density of  $\text{H}_3^+$  varies approximately as the square root of the input energy (Achilleos *et al.* 1998), the column density derived for the Saturn spectrum is consistent with the ratio of cronian to jovian energy inputs. What then causes the relatively low emission from Saturn is a combination of lower input fluxes, leading to lower  $\text{H}_3^+$  column densities, coupled with lower temperatures. This suggests it is not necessary to invoke additional chemical depletion to explain the observations (see Atreya 1986). The lower ionospheric temperatures—presumably resulting from lower input energies—suggest that  $\text{H}_3^+$  emission may not be as effective a coolant as is the case for Jupiter. But a detailed energy balance of Saturn is still awaited.

JIM Jupiter model,  $a = 5.0$  AU

(subsolar longitude: 328, time: 4.911 Jovian days)



GIM exoplanet model,  $a = 0.5$  AU  
(subsolar longitude: 340, time: 4.944 Jovian days)

GIM exoplanet model,  $a = 0.05$  AU  
(subsolar longitude: 344, time: 4.956 Jovian days)

Figure 6. Effect of increasing the insolation to JIM to produce a giant ionosphere model (GIM) to simulate exoplanets. The effect is reported in terms of decreasing distance to a Sun-like star.

### (b) *Uranus*

Although it is roughly twice as far away from Earth as Saturn,  $\text{H}_3^+$  emission from Uranus was actually detected prior to that of the nearer planet (Trafton *et al.* 1993). Uranus is a peculiar planet, with its rotation axis in the plane of the Ecliptic (the plane in which the planets orbit the Sun) and its magnetic field strongly offset from both the rotational poles and the centre of the planet (Connerney *et al.* 1987). In strong contrast with Jupiter, Uranian emission shows little sign of bright auroral regions. Lam *et al.* (1997b) concluded that any auroral enhancement amounted to no more than *ca.* 20% of the total  $\text{H}_3^+$  output from the planet. Typically, rotational tem-



peratures ranging from *ca.* 630 to 760 K (see Trafton *et al.* (1999) for a major study of the H<sub>2</sub> and H<sub>3</sub><sup>+</sup> emission of Uranus) are found, with vibrational temperatures—found by ratioing lines in the overtone spectrum to those in the fundamental—from 490 to 680 K. Trafton *et al.* (1999) reported that the total emission from the sunlit hemisphere of the planet was  $2.2 \times 10^{11}$  W in 1992, close to the last maximum in solar activity, falling to half this value in 1995, close to the solar minimum. They concluded that Uranian H<sub>3</sub><sup>+</sup> emission was dependent upon solar activity much more directly than has been reported for Jupiter (Baron *et al.* 1996). Recent measurements show the emission levels increasing once more with the rise in solar activity (L. M. Trafton *et al.*, unpublished data).

Additionally, Trafton *et al.* (1999) found that the total infrared emission from H<sub>3</sub><sup>+</sup> was comparable with, or maybe only 50% of, that of molecular hydrogen; this again is a contrast with Jupiter, where H<sub>3</sub><sup>+</sup> emission is the main coolant in the upper atmosphere. However, it may be that the bulk of the H<sub>2</sub> emission comes from deeper in the atmosphere: the Uranian homopause is lower than that of Jupiter. The distribution of the two molecules across the planetary disc is by no means similar: while H<sub>3</sub><sup>+</sup> emission appears to be peaked close to the sub-solar point on the planet, H<sub>2</sub> emission shows strong brightening at the limbs of the planet (figure 5). Trafton *et al.* (1999) attributed this difference to H<sub>2</sub> emission being formed in a thick shell reaching right down to the 10 μbar pressure level, while that from H<sub>3</sub><sup>+</sup> came from a thin shell, which extended no further than the 1 μbar level, much more susceptible to effects of increased insolation at the sub-solar point. It may be that all of the H<sub>3</sub><sup>+</sup> emission from Uranus results from the formation of this molecule by solar EUV ionization. Measurements of equatorial H<sub>3</sub><sup>+</sup> column densities on Jupiter (Lam *et al.* 1997*a*; Miller *et al.* 1997) and modelling (Achilleos *et al.* 1998) are consistent in showing values of a few  $\times 10^{15}$  m<sup>-2</sup>, and, at four times the distance from the Sun, Uranian values should be *ca.* 25% of this. Trafton *et al.* (1999) reported values between  $1.43$  and  $4.28 \times 10^{15}$  m<sup>-2</sup>. These are possibly a little too high to result solely from solar EUV. But the magnetic field of Uranus is such that relatively high particle precipitation levels, derived from the solar wind, are also possible at the sub-solar point (Hudson *et al.* 1989).

### (c) *Extra-solar planets*

The discovery in the last few years of more than 20 planets orbiting around stars close to our own Solar System has transformed the field of planetary science, bringing it right into the centre of contemporary astronomy. The technique used almost exclusively so far—looking for Doppler shifts in the spectra of the central stars that can be accounted for by the gravitational attraction of orbiting bodies (Mayor & Queloz 1995; Marcy & Butler 1996; Cumming *et al.* 1999)—reveals details about the orbital parameters and masses of the planets concerned, but little about their intrinsic nature. The Doppler-shift method, by its very nature, is most sensitive to large planets that orbit close to their star. The catalogue maintained by Schneider (<http://www.obspm.fr/planets>) shows many planets with masses similar to or greater than that of Jupiter. Recently, two groups have reported detecting a planet transiting in front of the Sun-like star HD 209458 (Charbonneau *et al.* 2000; Henry *et al.* 2000), which give, additionally, the radius, estimated to be between  $1.27$  and  $1.42R_J$ . And, even more excitingly, Cameron *et al.* (1999) have detected starlight

reflected from an  $8M_J$ , blue-green planet orbiting Tau Bootes. The way to study planetary atmospheres in systems other than our own is opening up at the beginning of the new millennium.

So what might conditions be like on these (super-)Jupiters, which appear to have spiralled in towards their central stars to a position of blistering proximity? We have used JIM to simulate the effect of bringing our own Jupiter in towards the Sun (figure 6). At 5 AU, its present orbit, the jovian column density of  $H_3^+$  at the sub-solar point due to insolation alone is between  $3$  and  $6 \times 10^{15} \text{ m}^{-2}$ ; at 0.5 AU, this increases to between  $6$  and  $10 \times 10^{16} \text{ m}^{-2}$ ; and at 0.05 AU, the orbit of the planet circling Tau Bootes, the value is *ca.*  $10^{18} \text{ m}^{-2}$ . But this figure is likely to be a considerable underestimate, since it does not allow for the expansion of the atmosphere (seen by Charbonneau *et al.* (2000) and Henry *et al.* (2000)), resulting from the increase in temperature, which M. Mumma (unpublished data) puts at greater than 2000 K, and the greater depth of the planet's atmosphere, likely from the increased mass. Nor does it allow for the increased ionization resulting from the enhanced stellar wind. It has been estimated that  $H_3^+$  emission lines in both the *K* ( $2 \mu\text{m}$ ) and *L/L'* ( $3\text{--}4 \mu\text{m}$ ) windows may produce fluxes of a few  $\times 10^{-21} \text{ W m}^{-2}$  on Earth as a result (S. Miller, unpublished data). This value makes their detection problematic, but not impossible, with existing ground-based infrared facilities. The prospect of detecting molecular emission from extra-solar planets in the not too distant future will allow us to provide detailed answers to questions about the formation and evolution of planetary systems in general.

#### 4. Conclusions

The first extra-terrestrial spectrum of  $H_3^+$  was an accidental bonus of the search for thermospheric emission from Jupiter. In the decade that followed, spectroscopic studies have used this ion to reveal vital information about the thermal structure and dynamics of the upper atmosphere of the giant planets. Such studies are naturally complementary to those making use of high-resolution imaging.  $H_3^+$  planetary studies have now truly come of age. The challenges of the future include making the measurement of ion winds a routine technique for probing the transport of energy in the ionosphere/thermosphere and the way in which this region couples to planetary magnetospheres, and the detection of  $H_3^+$  emission from extra-solar planets.

It is a pleasure to acknowledge the expert assistance of staff at the United Kingdom Infrared Telescope and the NASA Infrared Telescope Facility, both located on Mauna Kea, Hawaii. Without their help, this work would not have been possible. This work was supported by the UK Particle Physics and Astronomy Research Council.

#### References

- Achilleos, N., Miller, S., Tennyson, J., Aylward, A. D., Mueller-Wodarg, I. & Rees, D. 1998 JIM: a time-dependent, three-dimensional model of Jupiter's thermosphere and ionosphere. *J. Geophys. Res.* **103**, 20 089–20 112.
- Achilleos, N., Miller, S., Prangé, R. & Dougherty, M. K. 2000 A dynamical model of Jupiter's auroral electrojet. *New J. Phys.* (Submitted.)
- Atreya, S. K. 1986 *Atmospheres and ionospheres of the outer planets and their satellites*, pp. 139–143. Springer.

- Atreya, S. K. & Donahue, T. M. 1976 Model ionospheres of Jupiter. In *Jupiter* (ed. T. Gehrels), pp. 304–310. Tucson, AZ: University of Arizona Press.
- Atreya, S. K., Waite Jr, J. H., Donahue, T. M., Nagy, A. F. & McConnell, J. C. 1984 Model ionospheres of Saturn. In *Saturn* (ed. T. Gehrels), pp. 239–251. Tucson, AZ: University of Arizona Press.
- Ballester, G. E. (and 21 others) 1996 Time-resolved observations of Jupiter's far-ultraviolet aurora. *Science* **274**, 409–413.
- Baron, R., Owen, T., Connerney, J. E. P., Satoh, T. & Harrington, J. 1996 Solar wind control of Jupiter's H<sub>3</sub><sup>+</sup> auroras. *Icarus* **120**, 437–442.
- Cameron, A. C., Horne, K., Penny, A. & James, D. 1999 Probable detection of starlight reflected from the giant exoplanet orbiting  $\tau$  Bootes. *Nature* **402**, 751–756.
- Charbonneau, D., Brown, T. M., Latham, D. W. & Mayor, M. 2000 Detection of planetary transits across a Sun-like star. *Astrophys. J.* **529**, L45–L48.
- Clarke, J. T., Weaver, H. A., Feldman, P. D., Moos, H. W., Fastie, W. G. & Opal, C. B. 1980 Spatial imaging of hydrogen Lyman alpha emission from Jupiter. *Astrophys. J.* **240**, 696–701.
- Clarke, J. T., Gladstone, G. R. & ben Jaffel, L. 1981 Jupiter's dayglow H Ly $\alpha$  emission profile. *Geophys. Res. Lett.* **18**, 1935–1938.
- Clarke, J. T. (and 20 others) 1996 Far-ultraviolet imaging of Jupiter's aurora and the 'Io footprint'. *Science* **274**, 404–409.
- Clarke, J. T. (and 11 others) 1998 Hubble Space Telescope imaging of Jupiter's UV aurora during the Galileo orbiter mission. *J. Geophys. Res.* **103**, 20217–20236.
- Connerney, J. E. P., Acuna, M. H. & Ness, N. F. 1987 The magnetic field of Uranus. *J. Geophys. Res.* **92**, 329–345.
- Cumming, A., Marcy, G. W. & Butler, R. P. 1999 The Lick Planet Search: detectability and mass thresholds. *Astrophys. J.* **526**, 890–915.
- de Bergh, C., Martin, A., Owen, T., Gautier, D., Maillard, J.-P., Lutz, B. L. & Drossart, P. 1992 Paper presented at *Workshop on Variable Phenomena in jovian Planetary Systems, Anapolis, MD, 13–16 July 1992*.
- Drossart, P. (and 11 others) 1989 Detection of H<sub>3</sub><sup>+</sup> on Jupiter. *Nature* **340**, 539–541.
- Feldman, P. D., McGrath, M. A., Moos, H. W., Durrance, S. T., Strobel, D. F. & Davidsen, A. F. 1993 The spectrum of the jovian dayglow observed at 3 Å resolution with the Hopkins Ultraviolet Telescope. *Astrophys. J.* **406**, 279–284.
- Geballe, T. R., Jagod, M.-F. & Oka, T. 1993 Detection of H<sub>3</sub><sup>+</sup> infrared emission lines in Saturn. *Astrophys. J.* **410**, L109–L112.
- Gross, S. H. & Rasool, S. I. 1964 The upper atmosphere of Jupiter. *Icarus* **3**, 311–322.
- Hamilton, D. C., Gloeker, G., Krimigis, S. M., Bostrom, C. O., Armstrong, T. P., Axford, W. I., Fan, C. Y., Lanzerotti, L. J. & Hunten, D. M. 1980 Detection of energetic hydrogen molecules in Jupiter's magnetosphere by Voyager 2: evidence for an ionospheric plasma source. *Geophys. Res. Lett.* **7**, 813–816.
- Henry, G. W., Marcy, G. W., Butler, R. P. & Vogt, S. S. 2000 A transiting '51 Peg-like' planet. *Astrophys. J.* **529**, L41–L44.
- Hill, T. W. 1979 Inertial limit on corotation. *J. Geophys. Res.* **84**, 6554–6558.
- Hudson, M. K., Clarke, J. T. & Warren, J. A. 1989 Ionospheric dynamo theory for production of far ultraviolet emissions on Uranus. *J. Geophys. Res.* **94**, 6517–6522.
- Kim, Y. K., Fox, J. L. & Porter, H. S. 1992 On H<sub>3</sub><sup>+</sup> density profiles in the jovian auroral ionosphere. *J. Geophys. Res.* **87**, 6093–6101.
- Lam, H. A., Achilleos, N., Miller, S., Tennyson, J., Trafton, L. M., Geballe, T. R. & Ballester, G. E. 1997a A baseline spectroscopic study of the infrared auroras of Jupiter. *Icarus* **127**, 379–393.
- Lam, H. A., Miller, S., Joseph, R. D., Geballe, T. R., Trafton, L. M., Tennyson, J. & Ballester, G. E. 1997b Variation in the H<sub>3</sub><sup>+</sup> emission of Uranus. *Astrophys. J.* **474**, L73–L76.

- Liu, W. & Dalgarno, A. 1996 The ultraviolet spectrum of the jovian dayglow. *Astrophys. J.* **462**, 502–518.
- Livengood, T. A., Moos, H. W., Ballester, G. E. & Prangé, R. 1992 Jovian ultraviolet activity, 1981–1991. *Icarus* **97**, 26–45.
- McConnell, J. C. & Majeed, T. 1991  $H_3^+$  in the jovian ionosphere. *J. Geophys. Res.* **92**, 8570–8578.
- Maillard, J.-P., Drossart, P., Watson, J. K. G., Kim, S. J. & Caldwell, J. 1990  $H_3^+$  fundamental band in Jupiter's auroral zones at high resolution from 2400 to 2900 inverse centimeters. *Astrophys. J.* **363**, L37–L41.
- Majeed, T. & McConnell, J. C. 1996 Voyager electron density measurements on Saturn: analysis with a time dependent ionospheric model. *J. Geophys. Res.* **101**, 7589–7598.
- Marcy, G. W. & Butler, R. P. 1996 A planetary companion to 70 Virginis. *Astrophys. J.* **464**, L147–L151.
- Matcheva, K. I. & Strobel, D. F. 1999 Heating of Jupiter's thermosphere by dissipation of gravity waves due to molecular viscosity and heat conduction. *Icarus* **140**, 328–340.
- Mayor, M. & Queloz, D. 1995 A Jupiter-mass companion to a solar-type star. *Nature* **378**, 355–359.
- Miller, S., Joseph, R. D. & Tennyson, J. 1990 Infrared emissions of  $H_3^+$  in the atmosphere of Jupiter at the 2.1 and 4.0 micron region. *Astrophys. J.* **360**, L55–L58.
- Miller, S., Achilleos, N., Ballester, G. E., Lam, H. A., Tennyson, J., Geballe, T. R. & Trafton, L. M. 1997 Mid-to-low latitude  $H_3^+$  emission from Jupiter. *Icarus* **130**, 57–67.
- Neale, L., Miller, S. & Tennyson, J. 1996 Spectroscopic properties of the  $H_3^+$  molecule: a new calculated linelist. *Astrophys. J.* **464**, 516–520.
- Oka, T. & Geballe, T. R. 1990 Observations of the fundamental 4 micron band of  $H_3^+$  in Jupiter. *Astrophys. J.* **351**, L53–L56.
- Prangé, R., Maurice, S., Harris, W. M., Rego, D. & Livengood, T. 1997 Comparison of IUE and HST diagnostics of the jovian aurora. *J. Geophys. Res.* **102**, 9289–9301.
- Prangé, R., Rego, D., Pallier, L., Connerney, J. E. P., Zarka, P. & Queinnee, J. 1998 Detailed study of FUV jovian auroral features with the post-COSTAR faint object camera. *J. Geophys. Res.* **103**, 20195–20216.
- Prinn, R. G. & Owen, T. 1976 The chemistry and spectroscopy of the jovian atmosphere. In *Jupiter* (ed. T. Gehrels), pp. 319–371. Tucson, AZ: University of Arizona Press.
- Rego, D., Achilleos, N., Stallard, T., Miller, S., Prangé, R., Dougherty, M. K. & Joseph, R. D. 1999 Supersonic winds in Jupiter's aurorae. *Nature* **399**, 121–124.
- Rego, D., Miller, S., Achilleos, N., Prangé, R. & Joseph, R. D. 2000 Latitudinal profiles of the jovian IR emission of  $H_3^+$  at 4  $\mu\text{m}$  with the NASA Infrared Telescope Facility: energy inputs and thermal balance. *Icarus*. (In the press.)
- Satoh, T. & Connerney, J. E. P. 1999 Jupiter's  $H_3^+$  emissions viewed in corrected jovimagnetic co-ordinates. *Icarus* **141**, 236–252.
- Satoh, T., Connerney, J. E. P. & Baron, R. 1996 Emission source model of Jupiter's  $H_3^+$  aurorae: a generalised analysis of images. *Icarus* **122**, 1–23.
- Seiff, A., Kirk, D. B., Knight, T. C., Young, L. A., Milos, F. S., Venkatapathy, E., Mihalov, J. D., Blanchard, R. C., Young, R. E. & Shubert, G. 1997 Thermal structure of Jupiter's upper atmosphere derived from the Galileo probe. *Science* **276**, 102–104.
- Stallard, T., Miller, S., Ballester, G. E., Rego, D., Joseph, R. D. & Trafton, L. M. 1999 The  $H_3^+$  latitudinal profile of Saturn. *Astrophys. J.* **521**, L149–L152.
- Trafton, L. M., Geballe, T. R., Miller, S. & Tennyson, J. 1993 Detection of  $H_3^+$  from Uranus. *Astrophys. J.* **405**, 761–766.
- Trafton, L. M., Miller, S., Geballe, T. R., Tennyson, J. & Ballester, G. E. 1999  $H_2$  and  $H_3^+$  emission from Uranus: the uranian thermosphere, ionosphere and aurora. *Astrophys. J.* **524**, 1059–1083.

- Trauger, J. T. (and 16 others) 1998 Saturn's hydrogen aurora: widefield and planetary camera 2 imaging from the Hubble Space Telescope. *J. Geophys. Res.* **103**, 20 237–20 244.
- Waite Jr, J. H., Cravens, T. E., Kozyra, J., Nagy, A. F., Atreya, S. K. & Chen, R. H. 1983 Electron precipitation and related aeronomy on the jovian thermosphere and ionosphere. *J. Geophys. Res.* **88**, 6143–6163.
- Waite Jr, J. H., Gladstone, G. R., Drossart, P., Cravens, T. E., Maurellis, A., Lewis, W. S., Mauk, B. & Miller, S. 1997 Jovian X-ray emission: key to understanding high temperatures measured by Galilean probe. *Science* **276**, 104–108.
- Yelle, R. V., Young, L. A., Vervack Jr, R. J., Young, R. E., Pfister, L. & Sandel, B. R. 1996 The structure of Jupiter's atmosphere: prediction for Galileo. *J. Geophys. Res.* **101**, 2149–2161.
- Young, L. A., Yelle, R. V., Young, R. E., Seiff, A. & Kirk, D. B. 1997 Gravity waves in Jupiter's thermosphere. *Science* **276**, 108–111.

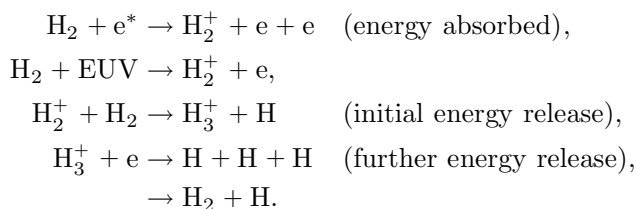
### Discussion

F. SCAPPINI (*Istituto di Spettroscopia Molecolare, Bologna, Italy*). You showed a spectrum of  $H_3^+$  taken with a vertical-slit spectrometer. What is the horizontal feature?

S. MILLER. The horizontal feature you see at all wavelengths across the spectrum of Jupiter in the polar regions is a 'polar haze'. This does not have a discrete line spectrum, but shows up as an enhanced continuum at the north and south pole. The assumption (I do not think anyone has actually modelled this) is that this haze is being formed by carbo-ion and carbo-radical reactions. These species are being created by the high fluxes of energetic particles that are precipitated at the jovian poles, and which are also responsible for the aurorae themselves.

J. B. A. MITCHELL (*PALMS, Université de Rennes, France*). Regarding your comment about  $H_3^+$  being a cooling agent in the ionosphere of Jupiter, the dissociative recombination of this ion is a violent event. For example, the dissociative recombination of  $NO^+$  is responsible for converting spark plug electrical energy into chemical energy, which ignites the fuel in a gasoline engine. For  $H_3^+$ , the fragments can carry away as much as 9 eV of kinetic energy. Electron degradation studies show that, for example, a 10 keV cosmic-ray electron loses much of its energy in the production of  $H_3^+$  in an interstellar cloud, and the released kinetic energy of the products serves to heat up the cloud. Has your model taken this effect into account?

S. MILLER. It is certainly true that the dissociative recombination of  $H_3^+$  is an energetic process. But it is not a primary source of energy to the jovian ionosphere/thermosphere. Instead, one can regard it as part of the process by which the energy of the precipitating particles (in the case of the auroral/polar regions) and the solar EUV flux, which are responsible for ionizing the atmosphere in the first place, is degraded into heat for the atmosphere. In a simplified schema one has:





Effectively, one is using the energy of precipitating particles/EUV photons to dissociate  $\text{H}_2$  molecules and collisionally heat the atmosphere via fast hydrogen atoms. (Typical fluxes are of the order of  $60 \mu\text{W m}^{-2}$  for solar EUV and  $1\text{--}10 \text{ mW m}^{-2}$  for particles.)

In the process, however, a column density of  $\text{H}_3^+$  of around  $n \times 10^{16} \text{ m}^{-2}$  in the auroral regions and  $m \times 10^{15} \text{ m}^{-2}$  is produced. These ions radiate strongly in the infrared at temperatures of *ca.* 1000 K, and, thus, radiate away the heat being produced by ionization and subsequent dissociative recombination. So our model takes these effects into account.

E. F. VAN DISHOECK (*Leiden Observatory, The Netherlands*). Can you comment on the  $\text{H}_3^+$  observations of the comet Shoemaker–Levy impact on Jupiter?

S. MILLER. As the comet crashed into the atmosphere of Jupiter, it was difficult to pick up the immediate effects on the ionosphere/thermosphere, which is where  $\text{H}_3^+$  emission is formed, because the  $\text{H}_3^+$  lines were swamped by very high intensity emission from hot methane in the stratosphere. This methane reached temperatures in excess of 2000 K, and some of it was blast accelerated to velocities up to  $100 \text{ km s}^{-1}$  (greater than the jovian escape velocity). So the immediate effects on the ionosphere were not visible in  $\text{H}_3^+$  emission. But three important effects were noted.

- (i) Between *ca.* 40 min and 1 h after the impact of some of the fragments, auroral emission was reported around latitudes of  $40\text{--}50^\circ$  in the Northern Hemisphere, corresponding to regions which were linked by magnetic fieldlines to the southern impact sites.
- (ii) After a few days, the ionosphere above the impact sites showed lower levels of  $\text{H}_3^+$  emission than normal. This was put down to chemical depletion of  $\text{H}_3^+$  by dust and metal-rich gas, which was mixed high into the ionosphere/thermosphere, above the normal homopause at around the  $1 \mu\text{bar}$  pressure level.
- (iii) After about a week, the normal southern auroral oval emission was found to be very ‘depressed’ such that the northern aurora appeared about 10 times brighter, instead of being of roughly equal intensity, as is usually the case. The northern auroral may have been brightened by about a factor of two, contributing to some of this effect. But, again, it was mainly attributed to the southern auroral  $\text{H}_3^+$  being chemically depleted by metal-rich gas and dust drifting from the impact sites into the circumpolar auroral region.